Proceedings of 9th International Symposium on Fluid-Structure Interactions, Flow-Sound Interactions, Flow-Induced Vibration & Noise
July 8-11, 2018, Toronto, Ontario, Canada

FIV2018-109

EXPERIMENTAL AND THEORETICAL ANALYSIS OF PERTURBATION GROWTH IN A LAMINAR JET.

Julia Zayko
Lomonosov Moscow State University
Moscow, Russia
zayko@imec.msu.ru

Sergey Teplovodskii
Lomonosov Moscow State University
Moscow, Russia
teplovodskii@imec.msu.ru

Anastasia Chicherina
Lomonosov Moscow State University
Moscow, Russia
chicherina@imec.msu.ru

Vladimir Trifonov
Lomonosov Moscow State University
Moscow, Russia
trifonovvl@mail.ru

Vasily Vedeneev
Lomonosov Moscow State University
Moscow, Russia
vasily@vedeneev.ru

Alexander Reshmin
Lomonosov Moscow State University
Moscow, Russia
alexreshmin@rambler.ru

ABSTRACT

Free jets and other shear flows often occur in nature and various technologies and are widely studied. Turbulent jets and their breakdown have been thoroughly studied over several decades in the context of many industrial applications, including mixing, combustion, noise generation and others.

Laminar jets are studied much less because of their immediate breakdown at normal conditions due to extremely small critical Reynolds number (~ 20*). In published experimental studies of free jets with the Reynolds number of* ~ 4000 *or greater, the transition to turbulence occurs near the orifice. However, in our previous work (Zayko et al., Physics of Fluids, 2018) we demonstrate a new method for the formation of free jets of 0.12 m diameter, with the Reynolds number of 10,000 and the laminar region length of 5 jet diameters.*

In this study, we investigate the perturbation growth in the long laminar jet. Perturbations are introduced through a metal oscillating foil strip. Results of the laser visualization are compared with theoretical predictions of the linear stability analysis. Impact of the perturbation frequency on the laminar portion length of the perturbed jet is in a reasonable agreement with the theoretical prediction.

INTRODUCTION

In the linear stability theory of shear flows, only a few classical results have been carefully tested experimentally. For the Blasius boundary layer, the first direct confirmation of theoretical prediction was conducted in [1], followed by several refined studies [2]. For the plane Poiseuille flow, experimental confirmation of theoretical neutral curve was done in [3,4]. Linear stability of Poiseuille flow in a round pipe for any Reynolds number can also be considered as experimentally verified, at least up to $Re \sim 100\,000$ [5].

However, for free shear flows, such as jets and wakes, situation is more complicated. In this case, an inviscid inflection-point mechanism, which is much stronger than the viscous instability in bounded flows, prevents the experimental observation of laminar flows at sufficiently large Reynolds numbers. The flow becomes turbulent immediately near its origin, and no perturbation growth study in laminar flow can be experimentally done.

Recently, we invented a novel method for the formation of laminar jet flows [6], which produces the jets of $D = 0.12$ m in diameter that stay laminar at the distance $5.5D$ from the orifice for the Reynolds number ~ 10000. Such characteristics provide a convenient way to investigate experimentally the perturbation growth in a free jet. In this study we start such an investigation. By comparing experimental results with theoretical stability analysis, we conclude that the perturbation growth follows the prediction of the linear stability theory up to the transition region of the jet.

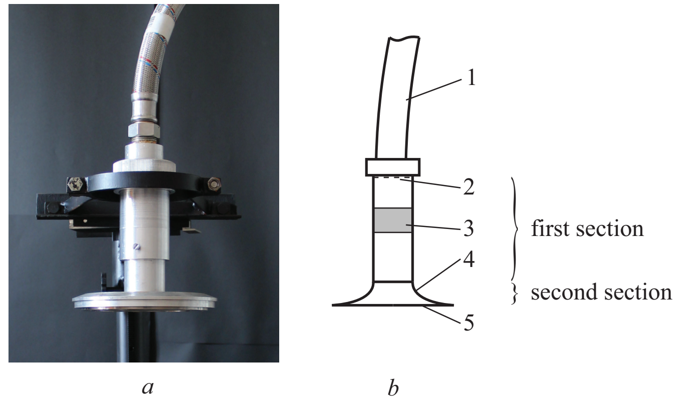

FIGURE 1: The photograph (*a*) and the draft (*b*) of the forming device. The pipeline from the gasholder (1), the perforated plate (2), the bushing with metal grids (3), the short diffuser (4) and the grid package (5).

EXPERIMENTAL APPARATUS

The experimental apparatus consists of the air supply device (pipeline), the forming device and the measurement system. The forming device's picture and the draft are shown in Fig. 1. Air flows from the gasholder to the forming device via the pipeline (1). Then it enters the forming device's first section through the short pipe. This section is the cylindrical channel of 0.04 m in diameter, where the flow is smoothened passing through the perforated plate (2), which also reduces the spatial scale of turbulent fluctuations. After the plate, the flow passes through a bushing with metal grids (3) of 0.05 m in length which is located at the distance of 0.03 m downstream from the perforated plate which reduces turbulence level. The second section of the forming device (short diffuser) is located at the distance of 0.06 m downstream from the bushing. At the length of 0.04 m, the flow expands to the diameter of 0.12 m through the diffuser (4) from which the jet flows to the atmosphere. For low incoming turbulence, the diffuser wall shape and the grid package (5) at the diffuser outlet provide low outcoming turbulence and 0.12 m diameter jet of the profile with almost constant velocity at the central core of 0.05 m in diameter. Details of the jet forming device, as well as measurements of the produced jet profiles at different Reynolds numbers can be found in [6].

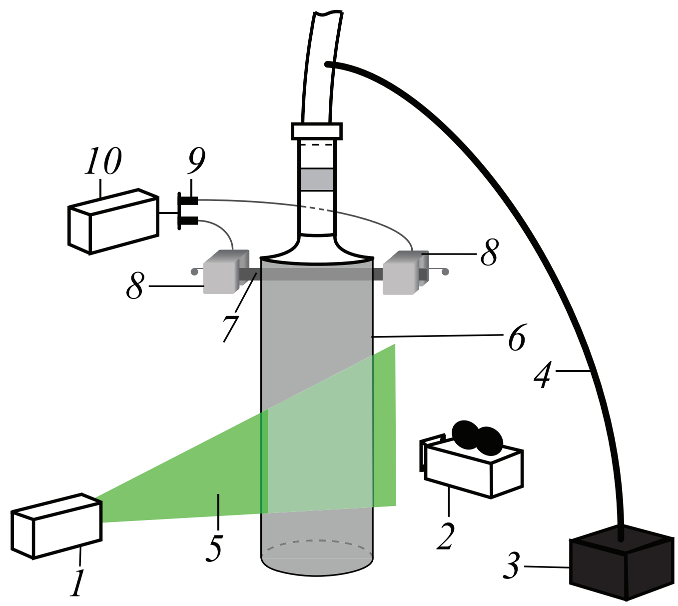

FIGURE 2: The draft of the visualisation system and the apparatus for the introduction of perturbations. Laser (1), video camera (2), aerosol generator (3), hose (4), laser light sheet (5) and jet (6). Oscillating foil strip (7), electromagnets (8), controller (9), power supply (10).

The jet visualization system is shown in Fig. 2. It consists of laser KLM-532 (1) and video camera Bonito CL-400B (2). Light-reflecting glycerin particles of ~ 10 μm in diameter are generated at the aerosol generator (3) and introduced to the flow through the hose (4). A segment of the jet is illuminated by the laser light sheet (5). The image is taken by the camera, whose optical axis is normal to the plane of the laser light sheet.

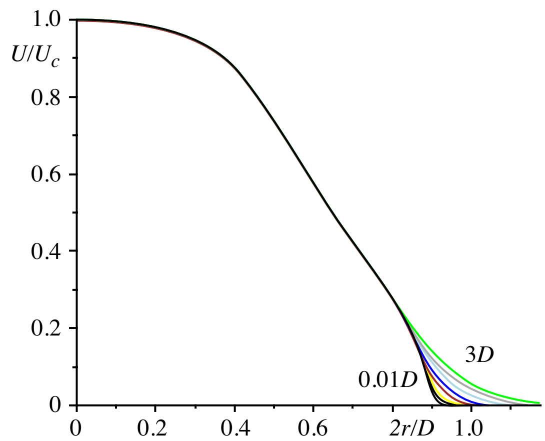

FIGURE 3: Mean velocity profile for $U_c = 1.5$ m/s ($Re = 5680$) at the distances $x/D = 0.01$, 0.04, 0.1, 0.25, 0.5, 1, 2, 3 from the orifice.

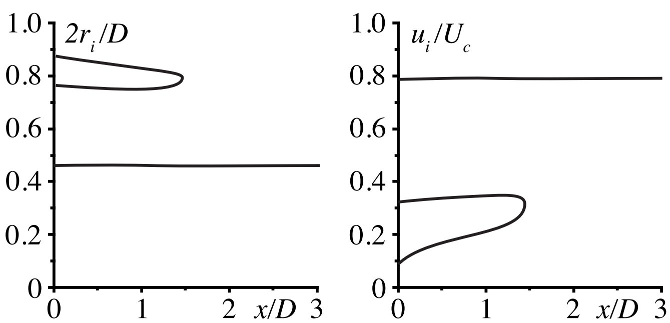

FIGURE 4: Location of the inflection points r_i and velocity at the inflection points $u_i = U(r_i)$ versus the distance from the orifice.

Perturbations are introduced into the jet by the oscillating foil strip (7) installed at the distance ~ 5 mm from the diffuser along its diameter (figure 2). The foil is placed into the slit of the electromagnets cores (8), and oscillates with the specified amplitude and frequency. The oscillation frequency is governed by the controller (9), whose voltage is supplied by the power source (10).

THEORETICAL STABILITY ANALYSIS OF A JET

Problem formulation

To theoretically analyse the evolution of artificial perturbations produced by the oscillating foil strip, we performed the spatial stability analysis of the jet. After the linearisation of the Euler equations around the steady jet flow with a given velocity profile $U(r)$, a single Rayleigh equation for the radial velocity perturbation for round jets in a cylindrical coordinate system can be derived [7]:

$$(U(r)-c)\frac{d}{dr}\left(\frac{r}{n^2+\alpha^2 r^2}\frac{d(rG(r))}{dr}\right) - (U(r)-c)\,G(r) - rG(r)\frac{d}{dr}\left(\frac{rU'(r)}{n^2+\alpha^2 r^2}\right) = 0, \quad (1)$$

where $G(r)$ is the amplitude of the radial velocity fluctuation: $u_r = iG(r)e^{i(\alpha x + n\varphi - \omega t)}$, $\alpha \in \mathbb{C}$ and $n \in \mathbb{Z}$ are axial and azimuthal wave numbers, $\omega \in \mathbb{R}$ is the frequency and $c = \omega/\alpha$ is the phase speed.

Perturbation $G(r)$ should satisfy two boundary conditions. First, at the jet boundary $r = 1$, the solution should match the zero-mean-velocity solution of the Rayleigh equation satisfying the radiation condition at $r = \infty$. This yields [6]

$$\frac{G'(r)}{G(r)} = \frac{K_n''(\alpha r)}{K_n'(\alpha r)}, \quad r = 1, \quad (2)$$

where $K_n'(\alpha r)$ is the derivative with respect to r of modified Bessel functions of the second kind. The second boundary condition at $r = 0$ is not as obvious and was discussed in detail in [7]. It can be summarised as

$$\begin{aligned} &G(0) = 0, \quad n = 0, \\ &G'(0) = 0, \quad n = 1, \\ &G(r) \sim r^{n-1}, \quad r \to 0, \quad n > 1\,. \end{aligned} \quad (3)$$

For each $\omega \in \mathbb{R}$, $n \in \mathbb{Z}$ the boundary-value problem for the Rayleigh equation (1), (2), (3) defines an eigenvalue problem to find $\alpha(\omega, n) \in \mathbb{C}$. Then the perturbation wave length is found as $\lambda = 2\pi/\operatorname{Re}\alpha$, and $\delta = -\operatorname{Im}\alpha$ is the perturbation growth rate.

For the sake of brevity, we consider here only axisymmetrical perturbation, $n = 0$. Clearly, perturbations that we have in the experiment are not axisymmetric; however, calculations show that for the first several non-zero n the eigenvalue analysis results are very close to those at $n = 0$ [6], so that the prediction obtained for $n = 0$ is valid for perturbations having several first components of the Fourier expansion in n. For arbitrary perturbations, qualitative agreement should be expected.

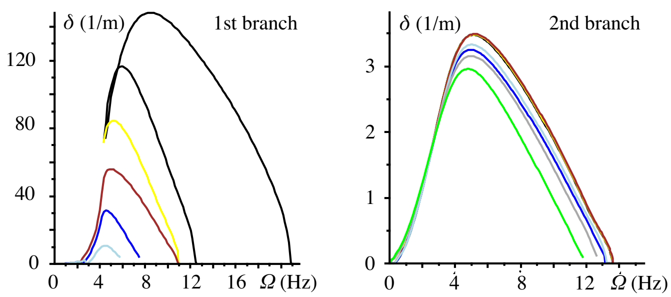

FIGURE 5: Theoretical spatial growth rate δ versus excitation frequency Ω at different distances from the diffuser (color coding corresponds to Fig. 3).

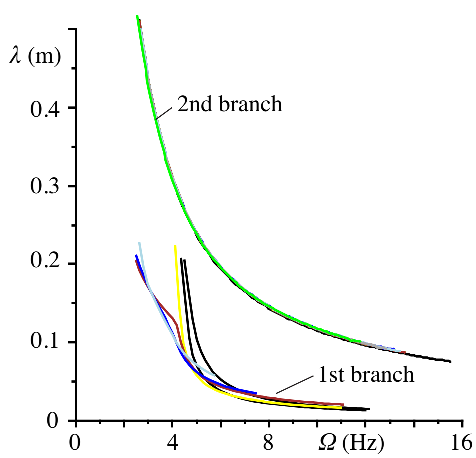

FIGURE 6: Theoretical wave length λ versus excitation frequency Ω.

Steady velocity profile

Mean velocity profiles calculated at different distances from the diffuser outlet are shown in Fig. 3. It is seen that due to the action of viscosity, initial steep drop of the velocity near the jet boundary becomes smoothened, whereas internal velocity distribution is almost not changed.

It is known that instability of free shear flows is driven by the inviscid inflection-point mechanism. For the case of round jets, the necessary instability condition for axisymmetric perturbations is given by the equation $(U(r)'/r)' = 0$, which is a generalization of inflection-point condition for planar flows to round flows. Below for the sake of brevity we will refer to the solutions of this equation as inflection points. Figure 4 shows the location of these points for the calculated mean profiles. It is seen that at the orifice there are three inflection points, but further downstream two of them merge and disappear, and only one inflection point closest to the jet axis remains at $x/D > 1.5$.

Results

For the velocity profiles near the orifice that have three inflection points, two branches of growing perturbations exist. The first branch is generated by two inflection points farthest from the jet axis. Further downstream, when these inflection points disappear, this branch of perturbations becomes damped. The second branch is generated by the infection point closest to the jet axis and remains growing arbitrarily far from the orifice. Calculated spatial growth rates (Fig. 5) show that while the first branch exists, its growth rate is much larger than of the second branch. But when this branch becomes damped, only the second branch generates instability. It is worth noting that the frequency range of growing perturbations is similar for both branches and corresponds to $0 < \Omega < 14$ Hz (except for extreme closeness to the orifice). The frequencies $\Omega = 4 - 6$ Hz corresponding to the maximum growth are also similar for both branches.

Figure 6 shows that wavelengths of the first branch are essentially shorter than of the second, which provides a clear way to experimentally distinguish observed perturbation branches.

EXPERIMENTAL STUDY OF PERTURBATION GROWTH

We study the perturbation growth in the laminar jet at the Reynolds number $Re = 5680$ (the velocity at the jet axis $U_c = 1.5$ m/s), for which the length of the laminar jet portion in the unperturbed condition is ~ 0.6 m. We aim to show that introduced perturbations with the frequencies from the range 4 – 6 Hz (corresponding to the theoretical maximum growth rates) grow spatially and yield the shortening of the laminar jet length, whereas, for the frequencies beyond this range the influence of the introduced perturbations on the laminar jet is not as essential.

Visualized flow patterns for various perturbation frequencies are shown in Fig. 7. In the absence of oscillations the foil presence in the jet does not affect the laminar region length. The visualization shows that the shortest laminar portion of the jet occurs for the frequencies 5 and 6 Hz. High frequencies (more than $10 - 15$ Hz) do not significantly shorten the laminar jet length. Values of the

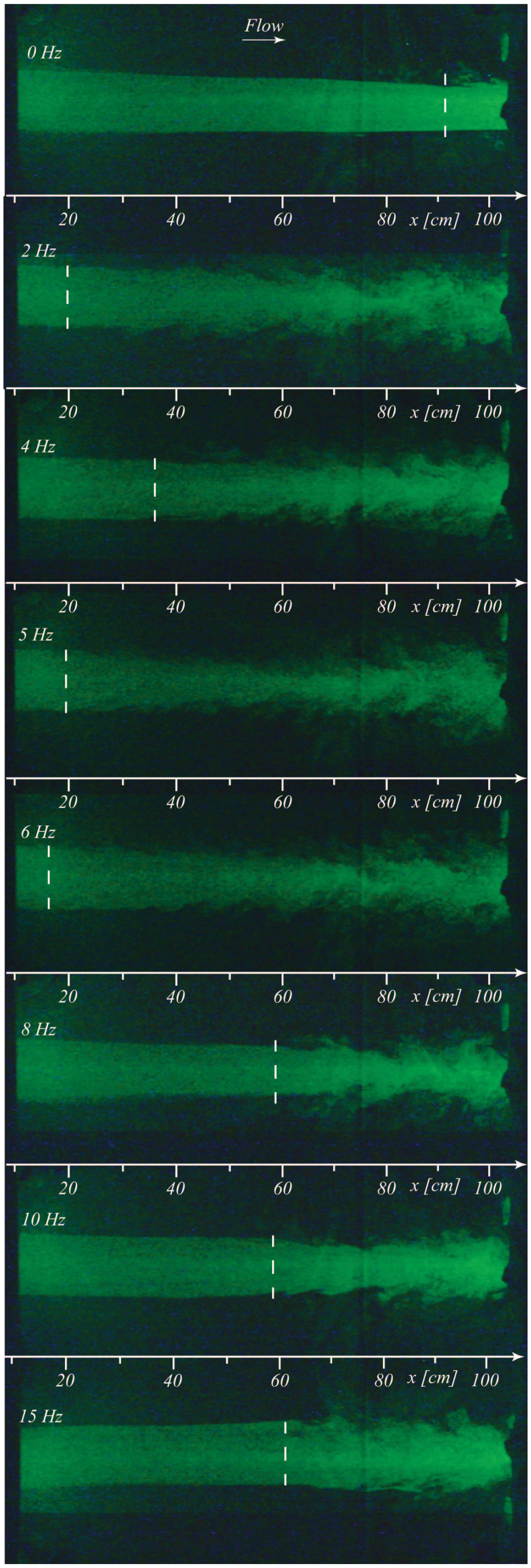

FIGURE 7: Impact of the oscillating foil strip on the laminar jet length for various oscillation frequencies. Visualization by glycerin particles and laser sheet.

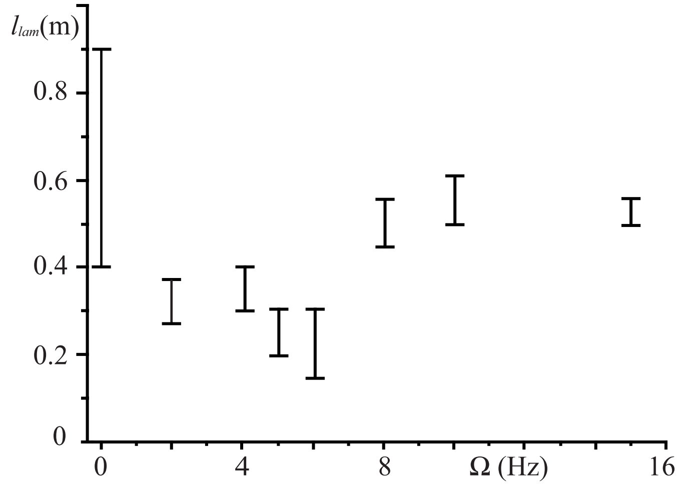

FIGURE 8: Length of the jet laminar region l_{lam} versus foil strip frequency Ω.

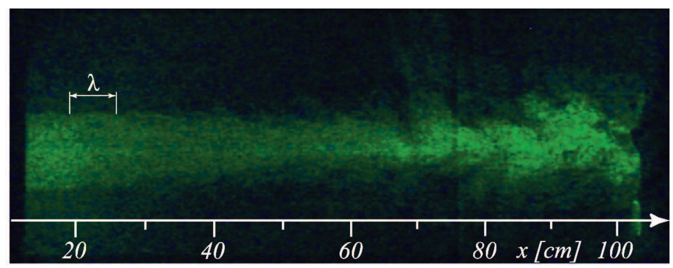

FIGURE 9: Wave length definition from the visualization of the jet perturbed with the frequency 4 Hz.

laminar jet lengths for various frequencies of the foil strip oscillations are shown in Fig. 8.

For each introduced frequency $(2,4,5,6,8,10,15$ Hz) the wave lengths of perturbations before the jet turbulisation are obtained from the visualization. We analyze the waves of small amplitude, near the jet origin (Fig. 9), because experimental wavelengths are compared with linear stability theory results.

Theoretically and experimentally obtained wavelengths are compared in Fig. 10. Experimental points are close to theoretical curves or higher, except for the results for the frequency 2 Hz. We see that experimental values are in agreement with modal theory predictions for the frequencies 4 and 5 Hz, which lies in the range of frequencies 4 – 6 Hz for the perturbations with maximum growth rates. For larger frequencies, experimental points are higher than corresponding theoretical curves. This is explained by non-axisymmetry of experimental perturba-

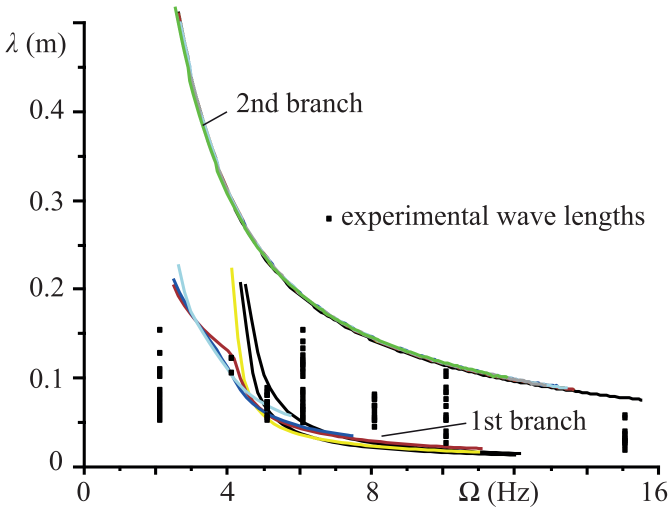

FIGURE 10: Theoretical (color curves) and experimental (black points) wavelengths λ versus excitation frequency Ω.

tions, whereas in theoretical investigation only axisymmetric perturbations are considered. For larger n, corresponding to non-axisymmetric perturbations, theoretical axial wave number α is smaller, that is, the wavelength λ is higher, which explains higher experimental values of the wavelengths in comparison with axisymmetric theory. From Fig. 10 we conclude that perturbations excited in experiment belong to the first, strong branch of perturbations, generated by the inflection point closest to the jet boundary, which is an agreement with theoretical expectations.

CONCLUSION

An axisymmetric laminar jet stability is theoretically analyzed for the jet profiles produced by the apparatus, which forms long laminar jets of 0.12 m in diameter for $Re = 2000 - 12000$. For the regime $Re = 5680$, two branches of growing perturbations exist, for both of them the frequency range for the fastest growing perturbations is $4 - 6$ Hz.

The influence of the perturbations produced the oscillating foil strip on the laminar jet is experimentally investigated. It is shown that experimental wavelengths of perturbations are in agreement with linear stability theory predictions. The shortest laminar region of the perturbed jet is observed for excitation frequencies 5 and 6 Hz, which is also in agreement with the theory.

As the next step, we plan to modify the apparatus for perturbation introduction to perform the experiments with axisymmetric perturbations for more accurate comparison of experimental and theoretical results.

ACKNOWLEDGMENTS

The work is supported by Russian Foundation for Basic Research Grant No. 18-38-00745.

REFERENCES

[1] Schubauer, G. B., Skramstad, H. K., 1948. “Laminar-Boundary-Layer Oscillations and Transition on a Flat Plate”. NACA-TR-909.

[2] Boiko, A.V., Westin, K.J.A., Klingmann, B.G.B., Kozlov, V.V., Alfredsson, P.H. 1994. “Experiments in a boundary layer subjected to free stream turbulence. Part 2. The role of TS-waves in the transition process”. *J. Fluid Mech.* **281**, 219–245.

[3] M. Nishioka, S. Iida, Y. Ichikawa. 1975. “An experimental investigation of the stability of plane Poiseuille flow”. *J. Fluid Mech.* **72**, part 4, 731–751.

[4] Kozlov V.V., Ramazanov, M.P., 1981. “An experimental investigation of the stability of Poiseuille flow”. *Izv. Akad Nauk SSSR, Tech. Sci.* **8**, 45–48.

[5] Eckhardt, B. 2009. “Introduction. Turbulence transition in pipe flow: 125th anniversary of the publication of Reynolds paper”. *Phil. Trans. R. Soc. A.* **367**, 449–455.

[6] Zayko, J., Teplovodskii, S., Chicherina, A., Vedeneev, V., Reshmin, A., 2018. “Formation of free round jets with long laminar regions at large Reynolds numbers”. *Physics of Fluids* 30, 043603 (2018).

[7] Batchelor, G.K., Gill, A.E. 1962. “Analysis of the stability of axisymmetric jets”. *J. Fluid Mech.* **14(4)**, 529–551.